Electronic structures of boron nitride nanotubes subjected to tension, torsion, and flattening: A first-principles DFT study

Yusuke Kinoshita* and Nobutada Ohno

Department of Computational Science and Engineering, Nagoya University, Furo-cho, Chikusa-ku, Nagoya 464-8603, Japan
and Department of Mechanical Science and Engineering, Nagoya University, Furo-cho, Chikusa-ku, Nagoya 464-8603, Japan

(Received 30 April 2010; revised manuscript received 13 July 2010; published 23 August 2010)

Electronic structures of (6,0), (8,0), and (10,0) single-walled boron nitride nanotubes (SWBNNTs) subjected to tension, torsion, and flattening are investigated using first-principles calculations. Energy bands and charge distributions of the SWBNNTs are calculated within the density-functional theory and forces required to deform the SWBNNTs are estimated using energy variation with deformation. Our calculations show that all the deformation modes decrease the energy gaps of the SWBNNTs because of a decrease in the conduction-band minimum (CBM) energy, which is caused by an overlap of CBM charge densities between circumferentially neighboring boron atoms. It is found that flattening with a force smaller than that applied for tension or torsion causes a larger decrease in energy gaps of the SWBNNTs and that the force required for flattening SWBNNTs is not unrealistic.

DOI: 10.1103/PhysRevB.82.085433 PACS number(s): 73.22.−f, 61.48.De, 71.15.Mb

I. INTRODUCTION

Boron nitride nanotubes (BNNTs) (Ref. 1) have a hexagonal ring structure,[2] similar to that of carbon nanotubes (CNTs),[3] and consist of alternately arranged boron and nitrogen atoms. Rubio *et al.*[4,5] theoretically predicted the existence of BNNTs in 1994 and then Chopra *et al.*[1] first synthesized multiwalled (MW) BNNTs in 1995. Since then, BNNTs have attracted the attention of many researchers owing to their important properties.[6] The mechanical strength[7,8] and thermochemical stability[9] of BNNTs are comparable to those of CNTs. For instance, experiments (using a thermal vibrational amplitude technique[7] and an electric field-induced resonance method[10]) and atomistic simulations (first-principles,[11–14] tight-binding,[15,16] and classical molecular mechanics[17–21] calculations) measured the Young's modulus of BNNTs to be in the range 0.7–1.2 TPa, which is close to that of CNTs (e.g., the average value is 1.8 TPa in Ref. 22 and 1.25 TPa in Ref. 23). In contrast, the electrical conductivity of BNNTs is completely dissimilar to that of CNTs. While CNTs become either metallic or semiconductive depending on the chirality, BNNTs are electrically insulating regardless of the diameter and chirality.[6] This is a notable characteristic of BNNTs that is different from CNTs. Therefore, BNNTs are expected to be used as electrical insulation coatings for conducting or semiconducting nanochains, nanowires, and nanotubes in severe conditions such as high temperatures and chemically hazardous environments.

However, a recent experimental study indicated that a bent MWBNNT was electrically conductive,[24] and a theoretical study showed that flattening decreased the energy gap of a zigzag single-walled (SW) BNNT.[25] These results indicate that the usefulness of BNNTs as nanocoatings might be lost under certain conditions (e.g., deformation caused by thermal stress or by a substrate constraint). Alternatively, BNNTs can be used in nanoelectronic devices by introducing deformation. In any case, our aim is to elucidate the electronic structures of deformed BNNTs.

The authors analyzed flattened SW and MWBNNTs using first-principles calculations[26] and clarified the mechanism of flattening-induced electronic changes in the BNNTs. Flattening calculations performed by the authors showed that the energy gaps of the BNNTs decreased with decreasing distance between circumferentially neighboring boron atoms in curved regions. Thus, because axial tension decreases the circumference of BNNTs as a result of Poisson contraction, it may also decrease the energy gap of BNNTs. In contrast, unless torsional buckling occurs, axial torsion may have little effect on the energy gap of BNNTs because it hardly changes the circumference of BNNTs.

In this study, to prove the above-mentioned hypotheses about BNNTs under tension and torsion and compare the magnitude of electronic changes in BNNTs under tension, torsion, and flattening, we investigate the electronic structures of SWBNNTs in the three deformation modes by first-principles density-functional-theory (DFT) calculations. We also estimate the forces required to deform the SWBNNTs in order to discuss the feasibility of deforming BNNTs. The results indicate that flattening with a smaller force than those applied for tension and torsion causes a larger decrease in the energy gap of the SWBNNTs and that the forces required to flatten the SWBNNTs are not unrealistic.

II. SIMULATION PROCEDURE

In this study, we focused on $(n,0)$ SWBNNTs with $n=6,8,10$, where (n,m) is the chiral index. The (n,m) tube has a diameter of $\sqrt{3}a\sqrt{n^2+nm+m^2}/\pi$, where a is the nearest interatomic distance between boron and nitrogen atoms. Figure 1 shows the simulation model of the (8,0) SWBNNT. The BNNT was located at the center of the unit cell so that the axial direction was parallel to the z direction. The cell size was $(\sqrt{3}an/\pi+2L_v)\times(\sqrt{3}an/\pi+2L_v)\times 3a$ with $a=0.145$ nm and $L_v=0.5$ nm, where L_v is the length of vacuum region in the unit cell. Although a three-dimensional periodic boundary condition was used, the cell sizes in the x and y directions were sufficiently large to avoid any interaction with neighboring image cells. We confirmed that they have little effect (less than 1%) on the total energy, charge

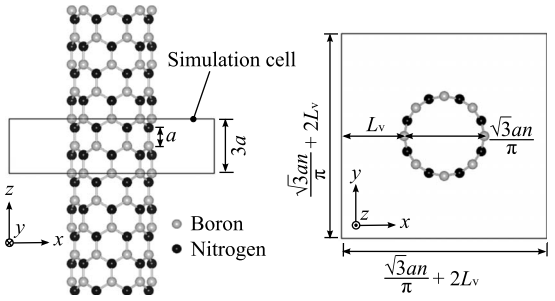

FIG. 1. Simulation model of (8,0) SWBNNT.

distribution and energy band structure of a deformed BNNT when they are larger than the tube diameter by 1.0 nm.

Atomic positions and the cell size in the z direction were first relaxed using the conjugate gradient method until atomic forces and the stress component, σ_{zz}, became less than 0.01 eV/Å and 0.01 GPa, respectively. After obtaining the equilibrium structure, tension, torsion, or flattening deformation was applied where atomic configurations were relaxed until their forces became less than 0.01 eV/Å.

In tension [Fig. 2(a)], the axial strain, ε_{zz}, was defined as

$$\varepsilon_{zz} = \frac{L_z - L_{z0}}{L_{z0}}, \tag{1}$$

where L_{z0} and L_z are the cell sizes in the z direction of unstretched and stretched BNNTs, respectively. In this study, ε_{zz} was in the range 0.00–0.10 with an increment of 0.02.

In torsion [Fig. 2(b)], atom i was rotated ϕ_i degrees about the z axis. ϕ_i was defined as

$$\phi_i = \theta z_i \tag{2}$$

$$\theta = \frac{360 N_\theta}{n N_z L_{z0}}, \tag{3}$$

where θ is the specific angle of twist, z_i is the z coordinate of atom i, N_θ is an integer, and N_z is the number of primitive unit cells in the z direction. The torsion angle must be an integral multiple (N_θ) of $360/n$ to fulfill the periodic boundary condition. In this study, the value of N_θ was 1 and that of N_z was in the range 3–5.

In flattening [Fig. 2(c)], compression in the x direction was applied by reducing the distance between imaginary walls. Once an atom contacts a wall, the atom is allowed to move only on the wall. The flattening ratio, η, was defined as

$$\eta = \frac{D_0 - D}{D_0}, \tag{4}$$

where D_0 is the tube diameter at equilibrium and D is the distance between the imaginary walls. In this study, η was in the range 0.00–0.50 with an increment of 0.05.

We conducted first-principles DFT calculations using the Vienna *ab initio* simulation package (VASP).[27,28] The wave functions were expanded in a plane-wave basis set with a cutoff energy of 350 eV. The ultrasoft pseudopotential proposed by Vanderbilt[29] was used and the exchange-correlation energy was evaluated by the generalized gradient approximation of Perdew and Wang.[30] The Brillouin zone integration was performed by the Monkhorst-Pack scheme[31] using a $1 \times 1 \times 4$ k-point mesh for atomic and electronic relaxations. After the relaxation, the energy band structure was obtained by calculating energy eigenvalues of 30 points on Γ-X line in the Brillouin zone.

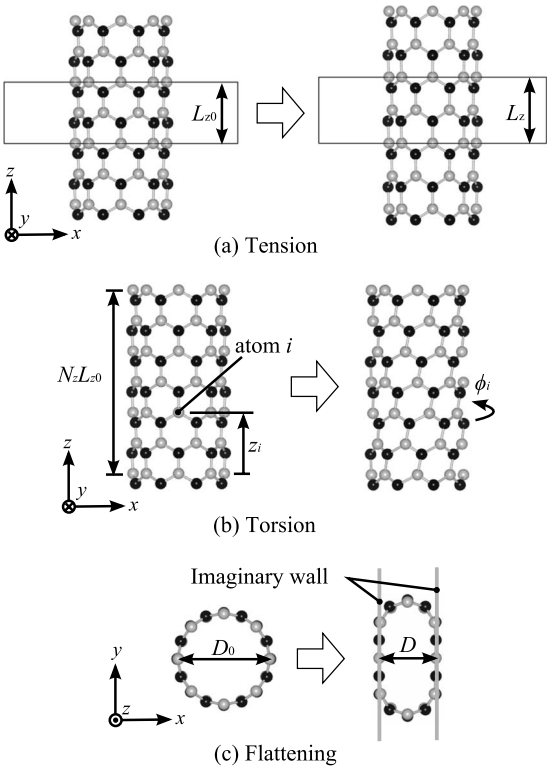

FIG. 2. Schematics of tension, torsion, and flattening of SWBNNT.

III. RESULTS AND DISCUSSION

A. Energy-band structures

It is well known that the DFT underestimates the energy gap. For a quantitative discussion of the energy gap, a modified theory such as the GW approximation (GWA) is necessary.[32–35] Nonetheless, previous studies on bulk hexagonal BN and an isolated BN sheet showed that the shape of the energy bands by the DFT is quite similar to that by the GWA except for the magnitude of the energy gap.[32,33] Thus, the DFT can qualitatively predict energy-band structures of BNNTs.

Figure 3 shows the change in the energy-band structures of the (8,0) SWBNNT under tension, torsion, and flattening. The (6,0) and (10,0) show a changing trend similar to the (8,0) band structure. A common feature among the three deformation modes is that both the valence-band maximum (VBM) and conduction-band minimum (CBM) are located at the Γ point ($k=0$) during the deformations. Another common feature is that the change in the energy of the VBM, E_{VBM}, is almost zero. Note that while the tension and flattening obviously decrease the energy of the CBM, E_{CBM}, the torsion hardly decreases E_{CBM}. The results suggest that all the three

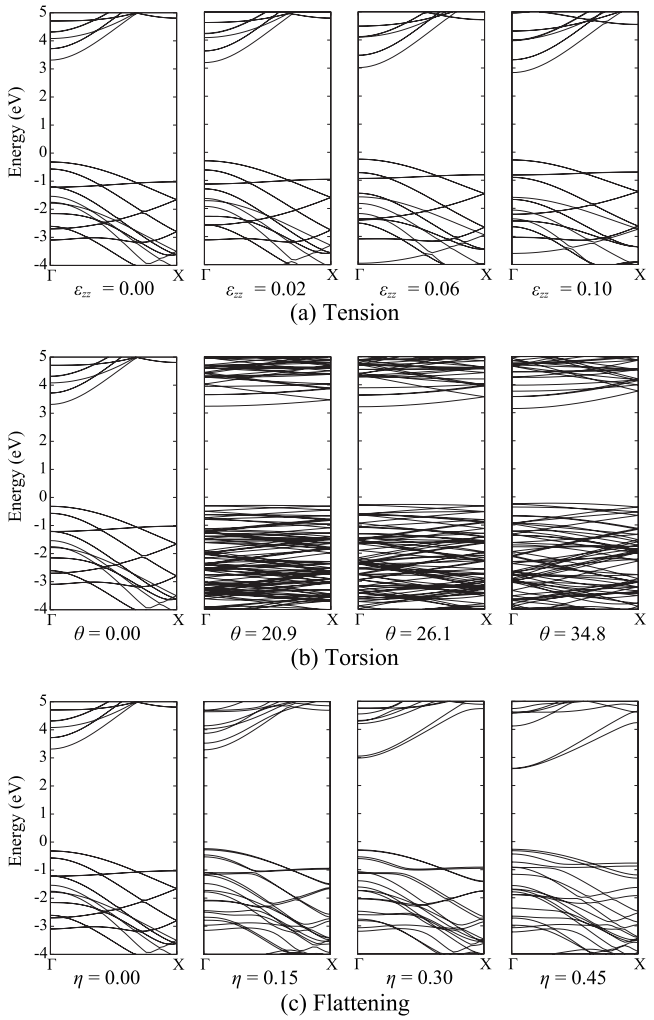

FIG. 3. Change in the band structure of an (8,0) SWBNNT. The origin of the energy scale is set at the Fermi level.

deformation modes decrease energy gaps, $E_g = E_{CBM} - E_{VBM}$, of SWBNNTs but torsion has less of an effect on the energy gap than tension and flattening, demonstrating that the hypotheses stated in Sec. I are correct.

Figure 4 shows the energy gaps of the (6,0), (8,0), and (10,0) SWBNNTs as a function of the axial strain, specific angle of twist, and flattening ratio. The energy gap of the (10,0) with $\theta = 41.7°/\text{nm}$ ($N_z = 5$) is not shown in the figure because it collapsed. Under tension and torsion except for $\theta = 20.8 - 27.8°/\text{nm}$ in the (10,0), the energy gap decreases almost linearly and the rate of decrease hardly depends on the diameter. In contrast, under flattening, the energy gap decreases quadratically or exponentially and the amount of decrease significantly depends on the diameter; a SWBNNT with the smaller diameter shows a larger decrease in the energy gap. It is also shown that flattening results in a few times larger decrease in the energy gap than tension and torsion.

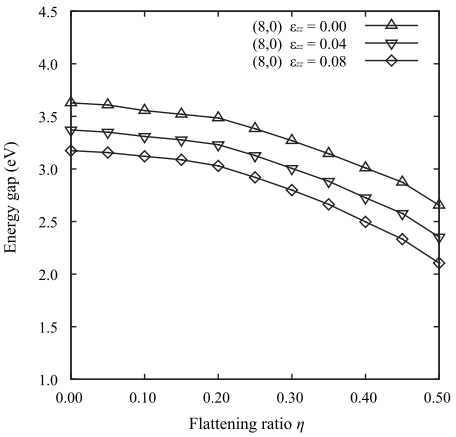

FIG. 5. Change in the energy gap of (8,0) SWBNNT under flattening following axial tension.

Although the discussion so far in this paper has dealt with the SWBNNTs under the three simple deformation modes, BNNTs would be subjected to combined deformation in their practical use. We therefore further analyzed the energy gap of the SWBNNTs subjected to flattening following axial tension (Fig. 5). It is found that preceding tension shifts an E_g-η curve downward without dramatic changes in its shape and that the extent of the shift almost corresponds to the energy gap decrease induced by simple tension [Fig. 4(a)]. This result suggests that the energy gap of the SWBNNTs under a combination of the three deformation modes can be deduced

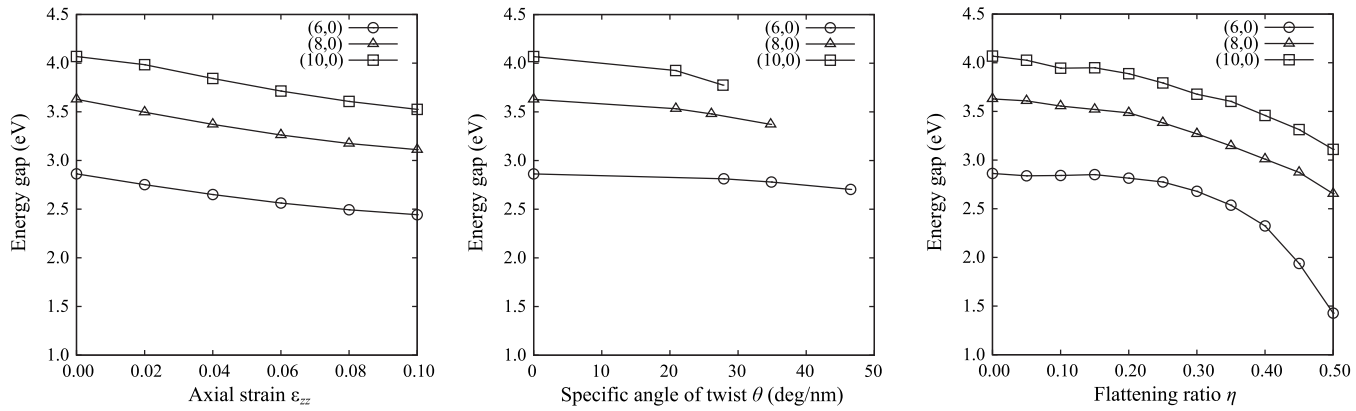

FIG. 4. Energy gaps of the SWBNNTs as a function of (a) axial strain, (b) specific angle of twist, and (c) flattening ratio.

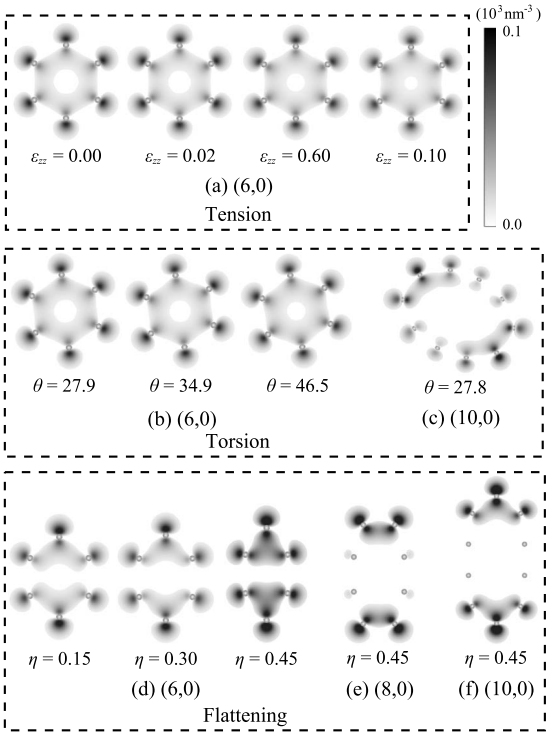

FIG. 6. Change in the CBM charge density. Cross sections passing through boron atoms are shown.

from Fig. 4. In the rest of this paper, therefore, only the simple deformation modes will be discussed.

B. Charge densities at the CBM

Here the mechanism of deformation-induced electronic changes in the SWBNNTs is discussed in terms of charge densities at the CBM (Fig. 6). The CBM is composed of boron-derived states. In fact, CBM charge densities are high around boron atoms while they are low around nitrogen atoms. We find that the π^* state (p_z orbitals of boron atoms) hybridizes with the σ^* state along a circumference passing through boron atoms under no deformation [Fig. 6(a), ε_{zz} =0.00] and that the tension, torsion, and flattening induce the change in the CBM state.

The authors have already discussed changes in CBM charge densities of BNNTs due to flattening:[26] charges are transferred from the flattened to the curved regions, resulting in an overlap of the charge densities and formations of electronic bonds between neighboring boron atoms in the curved regions [Fig. 6(d)]. It is this mechanism that results in the decrease in E_{CBM} in the flattened SWBNNTs. Comparing the three SWBNNTs with η=0.45 [Figs. 6(d)–6(f)], we see that the electronic bonds become stronger as the diameter becomes smaller. Therefore, a flattened SWBNNT with a smaller diameter shows a larger decrease in the energy gap.

Under tension [Fig. 6(a)], the tube curvature increases because of Poisson contraction, leading to the enhancement of π^*-σ^* hybridizations and the decrease in E_{CBM}. Figure 6(a) shows the narrowing white center area of zero-charge densities and the spreading gray area of π^*-σ^* hybridizations. The same is true for the torsion [Fig. 6(b)] but it induces less change in charge densities than tension [the size of the white center area changes little in Fig. 6(b)], resulting in a smaller decrease in the energy gap under torsion than under tension [Figs. 4(a) and 4(b)]. It should be noted that elastic buckling occurred at a θ between 20.8 and 27.8°/nm in the (10,0), leading to local flattening [Fig. 6(c)]. Therefore, the relation of E_g versus θ deviates from the linear decrease at θ of 20.8–27.8°/nm in the (10,0) [Fig. 4(b)]. It is obvious that the overlap of charge densities is much stronger under flattening than under tension or torsion. Therefore, the decrease in the energy gap in the former is much larger than in the latter.

C. Deformation forces

Figure 7 shows the deformation energy as a function of axial strain, specific angle of twist, and flattening ratio. The curves in tension, torsion, and flattening are fitted by cubic, quadratic, and quartic polynomials, respectively. The first and second derivatives of each curve provide the deformation force (Fig. 8) and the elastic modulus, respectively. Young's moduli of the (6,0), (8,0), and (10,0) are thus calculated to be 0.759 TPa, 0.794 TPa, and 0.811 TPa, respec-

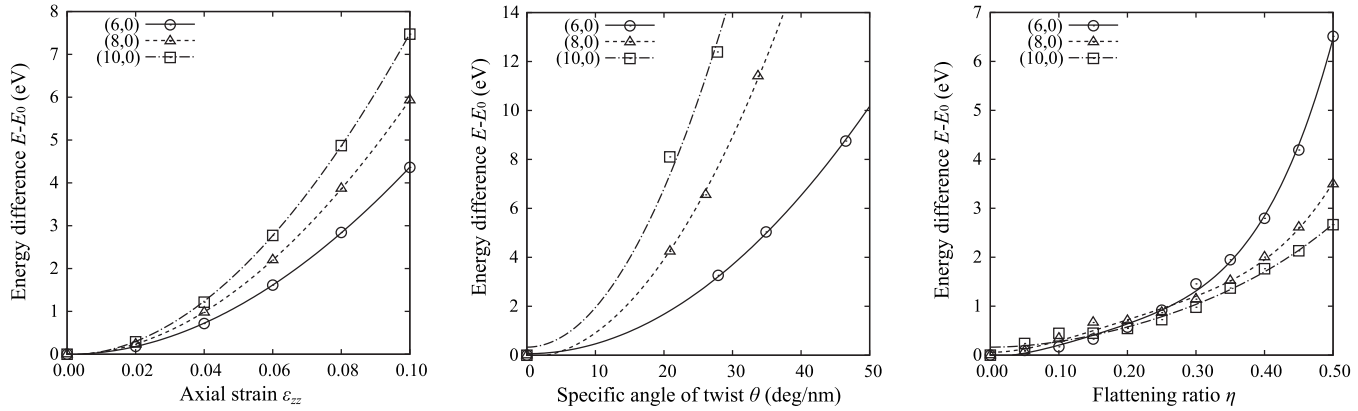

(a) Tension (b) Torsion (c) Flattening

FIG. 7. Deformation energy of the SWBNNTs as a function of (a) axial strain, (b) specific angle of twist, and (c) flattening ratio.

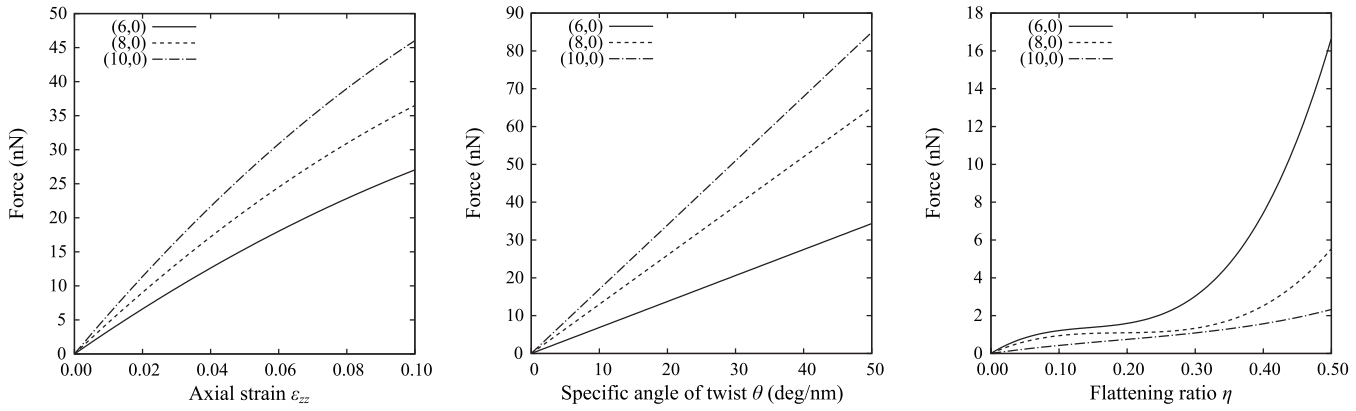

FIG. 8. Forces required to deform (6,0), (8,0), and (10,0) SWBNNTs.

tively. They are in good agreement with those measured in experiments (1.22 ± 0.24 TPa in Ref. 7 and 0.722 TPa in Ref. 10) and other first-principles calculations [e.g., in Ref. 14, 0.762 TPa, 0.785 TPa, and 0.803 TPa for (6,0), (8,0), and (10,0), respectively]. It is found in Fig. 8 that forces under flattening are smaller than under tension and torsion, because strong in-plane B-N covalent bonds prevent in-plane tension and torsion. It is also found that forces rapidly increase later under flattening. The rapid increase starts from around $\eta = 0.3$ and 0.4 in the (6,0) and (8,0), respectively, where the imaginary wall distances are 0.35 nm and 0.38 nm, respectively. Because the interlayer distance of hexagonal BNs and MWBNNTs is around 0.34 nm, the rapid increase would be attributed to the repulsive force between the two flattened regions.

Figure 9 shows the relationship between energy gap and deformation force. The three bands to the right illustrate the obtainable range of the energy gap by introducing tension, torsion, and flattening. In tension and torsion, a larger force is required for a larger tube to induce the same amount of energy gap decrease. The opposite is true in flattening, i.e., a larger force for a smaller tube. The key findings from Fig. 9 are that (i) the flattening with a force smaller than that applied for tension or torsion leads to the larger decrease in the energy gap and (ii) flattening offers a larger obtainable range of the energy gap than tension and torsion: 1.4–4.0 eV under flattening, 2.5–2.8 eV and 3.1–4.0 eV under tension, and 2.7–2.8 eV, 3.4–3.6 eV, and 3.8–4.0 eV under torsion. These findings indicate that flattening has the potential to enable BNNTs to be used as nanoelectronic devices. However, a valid question is whether flattening BNNTs is experimentally feasible.

In order to answer this question, we compare the estimated flattening forces with those of SWCNTs that Barboza *et al.*[36] have already experimentally succeeded in flattening by means of an atomic force microscopy (AFM) tip. Although they did not actually measure flattening forces of $(n,0)$ SWCNTs with $n \leq 10$, they proposed and validated a universal relationship among the applied force, SWCNT diameter, AFM tip radius, and flattening ratio

$$\frac{FD_0^{3/2}}{(2R)^{1/2}} = \frac{\alpha}{(1-\eta)^{3/2}}\left[\sqrt{2\eta+\eta^2} + tg^{-1}\left(\sqrt{\frac{\eta}{1-\eta}}\right)\right], \quad (5)$$

where R is the AFM tip radius and α is a constant ($=1.2 \times 10^{-18}$ J). Equation (5) indicates that the quantity $FD_0^{3/2}(2R)^{-1/2}$ should be universal to any SWCNT. They showed that all experimental data fall on a single curve obtained by Eq. (5) up to $\eta \simeq 0.4$. From Eq. (5) and the geometric contact conditions between a tube and an AFM tip, the flattening force per unit length of a (6,0) SWCNT ($D_0 = 0.470$ nm) is calculated to be 15.4 N/m when $\eta = 0.4$ and $R = 30$ nm. In contrast, from Fig. 8, that of the (6,0) SWBNNT ($=F/L_{z0}$) is estimated to be 16.8 N/m at $\eta = 0.4$. The results demonstrate that the flattening force is almost equal in SWCNTs and SWBNNTs, indicating that the same experiments as Barboza *et al.* would be feasible for SWBNNTs. The fact that CNTs and BNNTs almost have the same tube shape and size when their chiral indexes are the same ($a \simeq 0.142$ nm in CNTs and $a \simeq 0.145$ nm in BNNTs) also encourages the feasibility of flattening BNNTs. We therefore conclude that the flattening forces estimated are not

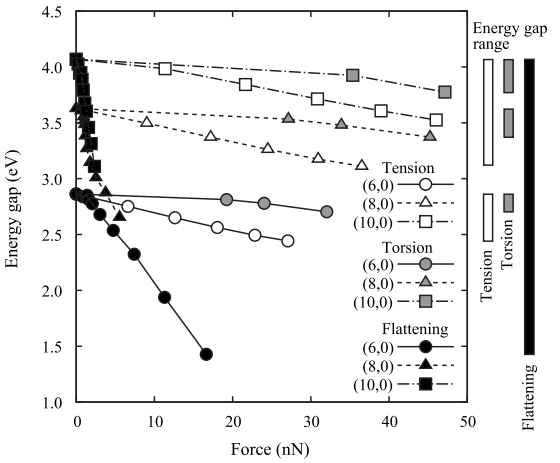

FIG. 9. Relationship between energy gap and force of (6,0), (8,0), and (10,0) SWBNNTs.

unrealistic and strongly expect that the same or similar experimental technique also applies to BNNTs.

IV. CONCLUSION

In this study, the electronic structures of $(n,0)$ zigzag SWBNNTs subjected to tension, torsion, and flattening were investigated by first-principles DFT calculations. The results revealed that the three deformation modes decrease the energy gaps of the SWBNNTs because of the decrease in the CBM energy caused by an overlap of CBM charge densities between circumferentially neighboring boron atoms. The key findings of this study are that flattening with a force smaller than that applied for tension or torsion causes a larger decrease in the energy gap and that the force required for flattening SWBNNTs is not unrealistic.

One of the issues to deal with in the future is to determine how defects and deformation concentration affect electronic structures of BNNTs. Electronic changes in BNNTs with such local nonuniformities will also be presented elsewhere in the near future.

ACKNOWLEDGMENTS

This work was supported in part by a Grant-in-Aid for Young Scientists (Start-up) under Grant No. 20810014 from Japan Society for the Promotion of Science and the Micro-Nano Global COE Program of Nagoya University.

*kinoshita@mech.nagoya-u.ac.jp

[1] N. G. Chopra, R. J. Luyken, K. Cherrey, V. H. Crespi, M. L. Cohen, S. G. Louie, and A. Zettl, Science **269**, 966 (1995).
[2] T. Oku, N. Koi, and K. Suganuma, J. Phys. Chem. Solids **69**, 1228 (2008).
[3] S. Iijima, Nature (London) **354**, 56 (1991).
[4] A. Rubio, J. L. Corkill, and M. L. Cohen, Phys. Rev. B **49**, 5081 (1994).
[5] X. Blase, A. Rubio, S. G. Louie, and M. L. Cohen, Europhys. Lett. **28**, 335 (1994).
[6] D. Golberg, Y. Bando, C. Tang, and C. Zhi, Adv. Mater. **19**, 2413 (2007).
[7] N. G. Chopra and A. Zettl, Solid State Commun. **105**, 297 (1998).
[8] T. Dumitrică, H. F. Bettinger, G. E. Scuseria, and B. I. Yakobson, Phys. Rev. B **68**, 085412 (2003).
[9] D. Golberg, Y. Bando, K. Kurashima, and T. Sato, Scr. Mater. **44**, 1561 (2001).
[10] A. P. Suryavanshi, M. F. Yu, J. Wen, C. Tang, and Y. Bando, Appl. Phys. Lett. **84**, 2527 (2004).
[11] K. N. Kudin, G. E. Scuseria, and B. I. Yakobson, Phys. Rev. B **64**, 235406 (2001).
[12] B. Akdim, R. Pachter, X. Duan, and W. W. Adams, Phys. Rev. B **67**, 245404 (2003).
[13] Y. J. Peng, L. Y. Zhang, Q. H. Jin, B. H. Li, and D. T. Ding, Physica E **33**, 155 (2006).
[14] B. Baumeier, P. Krüger, and J. Pollman, Phys. Rev. B **76**, 085407 (2007).
[15] E. Hernández, C. Goze, P. Bernier, and A. Rubio, Phys. Rev. Lett. **80**, 4502 (1998).
[16] E. Hernández, C. Goze, P. Bernier, and A. Rubio, Appl. Phys. A: Mater. Sci. Process. **68**, 287 (1999).
[17] C. Li and T. W. Chou, J. Nanosci. Nanotechnol. **6**, 54 (2006).
[18] V. Verma, V. K. Jindal, and K. Dharamvir, Nanotechnology **18**, 435711 (2007).
[19] J. Song, J. Wu, Y. Huang, K. C. Hwang, and H. Jiang, J. Nanosci. Nanotechnol. **8**, 3774 (2008).
[20] M. Griebel, J. Hamaekers, and F. Heber, Comput. Mater. Sci. **45**, 1097 (2009).
[21] M. Santosh, P. K. Maiti, and A. K. Sood, J. Nanosci. Nanotechnol. **9**, 5425 (2009).
[22] M. M. J. Treacy, T. W. Ebbesen, and J. M. Gibson, Nature (London) **381**, 678 (1996).
[23] A. Krishnan, E. Dujardin, T. W. Ebbesen, P. N. Yianilos, and M. M. J. Treacy, Phys. Rev. B **58**, 14013 (1998).
[24] X. Bai, D. Golberg, Y. Bando, C. Zhi, C. Tang, M. Mitome, and K. Kurashima, Nano Lett. **7**, 632 (2007).
[25] Y. H. Kim, K. J. Chang, and S. G. Louie, Phys. Rev. B **63**, 205408 (2001).
[26] Y. Kinoshita, S. Hase, and N. Ohno, Phys. Rev. B **80**, 125114 (2009).
[27] G. Kresse and J. Hafner, Phys. Rev. B **47**, 558 (1993).
[28] G. Kresse and J. Furthmuller, Phys. Rev. B **54**, 11169 (1996).
[29] D. Vanderbilt, Phys. Rev. B **41**, 7892 (1990).
[30] J. P. Perdew and Y. Wang, Phys. Rev. B **45**, 13244 (1992).
[31] H. D. Monkhorst and J. D. Park, Phys. Rev. B **13**, 5188 (1976).
[32] X. Blase, A. Rubio, S. G. Louie, and M. L. Cohen, Phys. Rev. B **51**, 6868 (1995).
[33] B. Arnaud, S. Lebègue, P. Rabiller, and M. Alouani, Phys. Rev. Lett. **96**, 026402 (2006).
[34] L. Wirtz, A. Marini, and A. Rubio, Phys. Rev. Lett. **96**, 126104 (2006).
[35] C. H. Park, C. D. Spataru, and S. G. Louie, Phys. Rev. Lett. **96**, 126105 (2006).
[36] A. P. M. Barboza, H. Chacham, and B. R. A. Neves, Phys. Rev. Lett. **102**, 025501 (2009).